Study of early leaf senescence in Arabidopsis thaliana by quantitative proteomics using reciprocal N-14/N-15 Labeling and difference gel electrophoresis

Hebeler, Romano; Oeljeklaus, Silke; Reidegeld, Kai E.; Eisenacher, Martin; Stephan, Christian; Sitek, Barbara; Stuehler, Kai; Meyer, Helmut E.; Sturre, Marcel J. G.; Dijkwel, Paul P.

Published in:
Molecular & Cellular Proteomics

DOI:
10.1074/mcp.M700340-MCP200

Document Version
Publisher's PDF, also known as Version of record

Publication date:
2008

Study of Early Leaf Senescence in *Arabidopsis thaliana* by Quantitative Proteomics Using Reciprocal $^{14}N/^{15}N$ Labeling and Difference Gel Electrophoresis*[S]

Romano Hebeler‡§, Silke Oeljeklaus‡§, Kai A. Reidegeld‡, Martin Eisenacher‡, Christian Stephan‡, Barbara Sitek‡, Kai Stühler‡, Helmut E. Meyer‡, Marcel J. G. Sturre¶, Paul P. Dijkwel¶, and Bettina Warscheid‡‖

Leaf senescence represents the final stage of leaf development and is associated with fundamental changes on the level of the proteome. For the quantitative analysis of changes in protein abundance related to early leaf senescence, we designed an elaborate double and reverse labeling strategy simultaneously employing fluorescent two-dimensional DIGE as well as metabolic ^{15}N labeling followed by MS. Reciprocal $^{14}N/^{15}N$ labeling of entire *Arabidopsis thaliana* plants showed that full incorporation of ^{15}N into the proteins of the plant did not cause any adverse effects on development and protein expression. A direct comparison of DIGE and ^{15}N labeling combined with MS showed that results obtained by both quantification methods correlated well for proteins showing low to moderate regulation factors. Nano HPLC/ESI-MS/MS analysis of 21 protein spots that consistently exhibited abundance differences in nine biological replicates based on both DIGE and MS resulted in the identification of 13 distinct proteins and protein subunits that showed significant regulation in *Arabidopsis* mutant plants displaying advanced leaf senescence. Ribulose 1,5-bisphosphate carboxylase/oxygenase large and three of its four small subunits were found to be down-regulated, which reflects the degradation of the photosynthetic machinery during leaf senescence. Among the proteins showing higher abundance in mutant plants were several members of the glutathione S-transferase family class phi and quinone reductase. Up-regulation of these proteins fits well into the context of leaf senescence since they are generally involved in the protection of plant cells against reactive oxygen species which are increasingly generated by lipid degradation during leaf senescence. With the exception of one glutathione S-transferase isoform, none of these proteins has been linked to leaf senescence before. ***Molecular & Cellular Proteomics 7:, 108–120.***

From the ‡Medizinisches Proteom-Center, Zentrum fuer klinische Forschung, Ruhr-Universitaet Bochum, Universitaetsstraβe 150, 44780 Bochum, Germany and ¶Molecular Biology of Plants, Groningen Biomolecular Sciences and Biotechnology Institute, University of Groningen, Kerklaan 30, 9751 NN, Haren, The Netherlands

Received, July 26, 2007, and in revised form, September 13, 2007.
Published, MCP Papers in Press, September 18, 2007, DOI 10.1074/mcp.M700340-MCP200

A major focus of proteome research is the simultaneous identification and quantification of proteins in cells, tissues, or organisms in dependence on the developmental stage, different physiological conditions, environmental influences, or genotypes. This quantitative, mass spectrometry (MS)[1]-based description of proteomes was facilitated by the development of various stable isotope labeling techniques that have since been applied to proteomics studies in a multitude of organisms (1, 2). In plant proteomics, however, the most frequently used method for comparative, quantitative studies so far has been two-dimensional PAGE (3). In traditional two-dimensional PAGE approaches, quantitative differences in protein abundance between biological samples are revealed by comparing spot patterns in individual gels based on densitometric analysis following silver or Coomassie Blue staining. Limitations of this method regarding reproducibility, sensitivity, and dynamic range of protein quantification were improved significantly by introducing the DIGE technology (4). The DIGE technique employs spectrally resolvable fluorescent cyanine dyes (CyDyes) to label proteins prior to separation by two-dimensional PAGE (5). Using the minimal labeling approach, two distinct protein samples are separately labeled with the fluorescent dyes Cy3 and Cy5, respectively, while an internal standard consisting of equal amounts of protein of all samples to be compared in a study is labeled with Cy2 (6). The internal standard is used for normalization of data and allows for both intra- and inter-gel comparison, thereby significantly reducing technical inconsistencies caused by gel-to-gel variations. This leads to improved accuracy and reproducibility of protein quantification and, provided that an appropriate number of independent experiments are performed, facilitates the statistically sound identification of differentially regulated proteins in biological samples. Despite the advantages resulting from the use of DIGE, however, this technique is subjected to the

[1] The abbreviations used are: *At*, *Arabidopsis thaliana*; cpr5, constitutive expressor of pathogenesis-related genes 5; CyDyes, cyanine dyes; FI, fluorescent intensity; GST, glutathione *S*-transferase; MLP, major latex protein; RP, reversed-phase; RuBisCO, ribulose 1,5-bisphosphate carboxylase/oxygenase; wt, wild-type.

same fundamental restrictions as traditional two-dimensional PAGE. It exhibits a strong bias against hydrophobic proteins such as membrane proteins and proteins with an extreme isoelectric point and/or molecular weight, for example. In addition, accurate relative protein quantification is impaired when two or more protein species are present in the same spot (7).

Stable isotope labeling of proteins or peptides combined with MS analysis represents an alternative strategy for accurate, relative quantification of proteins on a global scale. In this approach, proteins or peptides of two different samples are differentially labeled with stable isotopes, combined in equal ratio, and then jointly processed for subsequent MS analysis. Relative quantification of proteins is based on the comparison of signal intensities or peak areas of isotope-coded peptide pairs extracted from the respective mass spectra. Stable isotopes can be introduced either chemically into proteins/peptides via derivatization of distinct functional groups of amino acids or metabolically during protein biosynthesis. Metabolic labeling strategies are based on the *in vivo* incorporation of stable isotopes during growth of organisms. Nutrients or amino acids in a defined medium are replaced by their isotopically labeled (^{15}N, ^{13}C, or ^{2}H) counterparts eventually resulting in uniform labeling of proteins during the processes of cell growth and protein turnover (1). As a consequence, differentially labeled cells or organisms can be combined directly after harvesting. This minimizes experimental variations due to separate sample handling and thus facilitates relative protein quantification of high accuracy. Since metabolic labeling is best applicable to biological systems that can be maintained under controlled conditions, it has been predominantly applied to unicellular organisms such as bacteria (8) and yeast (9) as well as cell culture systems (10). However, the feasibility to label multicellular organisms such as *Caenorhabditis elegans*, *Drosophila melanogaster*, and a rat metabolically was shown as well (11, 12). Recently, increasing efforts have been made to adopt metabolic labeling for plant proteomics. Suspension cultures of *Arabidopsis thaliana* cells or *A. thaliana* plants grown in liquid culture were successfully labeled with either stable isotope-coded amino acids (13) or with ^{15}N (14–18).

In the present study, we used *A. thaliana* as model organism to gain deeper insights into early leaf senescence on the protein level. Leaf senescence is a highly regulated process in which nutrients from the senescing leaf are relocated to other parts of the plant and which eventually leads to leaf death (19). To identify changes in protein abundance related to early leaf senescence, we analyzed 16-day-old *A. thaliana* wild-type (wt) plants *versus* the onset of leaf death mutant *old1–1*. Compared with the wt, this mutant features a strong early leaf senescence phenotype (described in detail in (20–22)). After 16 days of growth, *A. thaliana* plants did not show visible signs of leaf senescence, *i.e.* yellowing of leaves. Expanding an approach reported by Kolkman *et al.* (23), we designed a double and reverse labeling strategy employing both two-dimensional DIGE and metabolic ^{15}N labeling for relative quantification of plant proteins. *A. thaliana* plants used in this work were grown on solid medium in a growth chamber simulating growth conditions as natural as possible. Reverse ^{14}N/^{15}N labeling experiments showed that quantitative incorporation of ^{15}N-isotopes (95%) had no adverse effects on plant development. The concomitant use of DIGE as alternative quantification technique provided us with a control to assess the consistency of the results obtained by both methods. Overall, we performed nine independent experiments, which led to the reliable identification of 13 different proteins or protein subunits with significant changes in abundance in the *old1–1* mutant plant. Ribulose 1,5-bisphosphate carboxylase/oxygenase large as well as three of its four small subunits showed decreased abundance in mutant plants. Proteins found to be up-regulated were, among others, several isoforms of the glutathione S-transferase (GST) family class phi and quinone reductase. These proteins are generally known to be involved in the detoxification of reactive oxygen species (24, 25).

EXPERIMENTAL PROCEDURES

Growth and Metabolic Labeling of Plants Using ^{14}N/^{15}N Isotopes—A. thaliana accession Landsberg erecta wt and *old1–1* mutant plants were grown under standard conditions (22 °C, 60–70% relative humidity, and 16 h of light). For metabolic labeling with ^{15}N, seeds were sown onto 19-cm Petri dishes containing stone wool (Grodan BV, Roermond, The Netherlands) wetted with ^{15}N-medium consisting of 0.75 mM $MgSO_4$, 3 mM $K^{15}NO_3$, 0.5 mM KH_2PO_4, 1.5 mM $CaCl_2$, and 0.11 mM $^{15}NH_4{}^{15}NO_3$ supplemented with Hoagland's micronutrients (26). ^{15}N-labeled salts were purchased from Cambridge Isotope Laboratories Inc. (Andover, MA) and were >98% enriched in ^{15}N. The Petri dishes were kept at 4 °C for 3 to 7 days and were then transferred to a growth chamber. During growth of the plants, the Petri dishes were kept humid with distilled water; medium was replenished every other week. After harvesting the seeds after 7–10 weeks of growth, they were sterilized with 1% bleach in 96% ethanol, washed twice with 96% ethanol, and dried. The sterilized seeds were then sown onto 15-cm Petri dishes containing medium solidified with 0.6% micro agar (Duchefa, Haarlem, The Netherlands). They were stratified at 4 °C for 3 to 7 days and subsequently transferred to the growth chamber. After 16 days of growth, the plants were frozen in liquid nitrogen, scraped off the dishes and stored at −80 °C prior to protein extraction. At this age, both *A. thaliana* wt and *old1–1* mutant plants did not show visible symptoms of leaf senescence under the growth conditions applied in this work. ^{14}N-labeled *A. thaliana* plants were grown in parallel under the same conditions in the presence of salts containing ^{14}N- and ^{15}N-isotopes at their natural abundance.

Preparation of Protein Extracts—Protein extracts were prepared according to Giavalisco *et al.* (27). In brief, frozen *A. thaliana* plants of an entire Petri dish (~500 mg) were supplied with 0.125 parts (w/w) of solution 1 [one tablet of Complete protease inhibitor (Roche Diagnostics, Mannheim, Germany) dissolved in 2 ml of 100 mM KCl, 20% (v/v) glycerol, and 50 mM Tris, pH 7.1] and 0.05 parts (w/w) of solution 2 [1 mM pepstatin A (Serva, Heidelberg, Germany) and 1.4 μM PMSF (AppliChem, Darmstadt, Germany) dissolved in ethanol]. Plants were ground to a fine powder in a mortar placed in liquid nitrogen. After centrifugation of the homogenate (30 min at 226,000 g and 4 °C), the supernatant containing the soluble proteins was collected and either

directly applied to two-dimensional PAGE or stored at −80 °C. Protein concentration was determined by amino acid analysis. After acidic hydrolysis of samples, the concentrations of free amino acids were analyzed by precolumn derivatization with 6-aminoquinolyl-*N*-hydroxysuccinimidyl carbamate using a Waters AccQFluor reagent kit (Waters Corporation, Milford, MA) (28, 29). Derivatives of amino acids were separated by reversed-phase (RP-) HPLC using a Waters AccQTag column (C_{18}, 15 cm × 2 mm inner diameter) on a Waters Alliance 2695 Separation Module. After fluorescence detection on a Waters 2475 Multi Fluorescence Detector, the concentrations of the separated amino acids were determined.

Labeling of Proteins Using CyDyes—Proteins were labeled with CyDyes according to the manufacturer's protocol (Amersham Biosciences/GE Healthcare). Before labeling, 54 mg of urea per 50 μl of protein sample (corresponding to ~130 μg of protein) were added (27); the pH was adjusted to 8.5 using 1 M Tris-base. Stock solutions of cyanine dyes (1 nmol/μl) were diluted with anhydrous dimethyl formamide (dimethylformamide, pro analysis; Sigma, St. Louis, MO) to 400 pmol/μl. 50 μg of protein were mixed with 400 pmol of cyanine dye (Cy2, Cy3, or Cy5; Amersham Biosciences/GE Healthcare), briefly centrifuged and incubated on ice in the dark for 30 min. The labeling reaction was stopped by addition of 1 μl of 10 mM L-lysine (Sigma) and incubation on ice for 10 min. In half of the experiments, proteins from wt and mutant plants were labeled with Cy3 and Cy5, respectively. In the other half of the experiments, fluorescent labeling was reversed. An internal standard generated by pooling equal amounts of proteins from each sample was labeled with Cy2. Differentially labeled samples were immediately combined in a 1:1:1 ratio and then subjected to protein separation by two-dimensional PAGE.

Separation of Differentially ^{14}N/^{15}N- and CyDye-labeled Proteins by Two-dimensional PAGE—Proteins were separated via two-dimensional PAGE following the protocol of Klose (30). To allow for relative quantitative analysis of proteins based on both fluorescent and metabolic labeling, extra 125 μg of protein per *A. thaliana* phenotype were added, resulting in a total of 400 μg protein per gel. 5 μl of 1.4 M DTT (BioRad, Munich, Germany) and 10 μl of the ampholyte mixture Servalyte 2–4 (Serva) were added per 100 μl of protein sample. IEF was performed according to Klose and Kobalz (31) in an IEF chamber produced in-house using tube gels (20 cm × 1.5 mm) that contained carrier ampholytes. Following IEF, the tube gels were ejected and incubated in equilibration buffer [125 mM Tris, 40% (w/v) glycerol, 3% (w/v) SDS, 65 mM DTT, pH 6.8] for 15 min. Gels were then washed three times with SDS-PAGE running buffer (25 mM Tris, 192 mM glycine, 0.2% SDS), placed on top of polyacrylamide gels (20 cm × 30 cm × 1.5 mm; 15.0% total acrylamide, 1.3% bisacrylamide), and fixed with 1.0% (w/v) agarose containing 0.01% (w/v) bromphenol blue (Riedel de-Haen, Seelze, Germany). SDS-PAGE was performed at 15 °C using a Desaphor VA 300 system (Desaga, Heidelberg, Germany) at a constant current flow of 75 mA for 15 min followed by a constant current flow of 200 mA for 6 to 7 hours.

Image Acquisition, Analysis, and Visualization of Proteins Separated by Two-dimensional DIGE—After gel electrophoresis, two-dimensional DIGE gels were scanned using the Typhoon 9400 Imager (Amersham Biosciences/GE Healthcare). Excitation wavelengths and emission filters were chosen specifically for each of the fluorescent dyes according to the manufacturer's user guide. Scans were acquired at a resolution of 100 μm. After cropping and filtering using the ImageQuant software (version 5.2, Amersham Biosciences/GE Healthcare), images were subjected to difference in-gel analysis and biological variation analysis using the DeCyder software, version 6.0 (Amersham Biosciences/GE Healthcare). Spot intensities were normalized based on the internal standard labeled with Cy2. Following image acquisition, proteins were visualized by colloidal Coomassie Brilliant Blue staining (32). ImageQuant 5.2 was used to convert two-dimensional DIGE images into the corresponding false color images.

In-gel Digestion of Proteins—Protein spots of interest were manually excised from the two-dimensional gel using a spot picker and transferred to glass mini-tubes. Gel spots were immediately destained by alternately incubating them with 20 μl of 10 mM ammonium hydrogen carbonate (NH_4HCO_3) and 20 μl of 5 mM NH_4HCO_3/50% ACN for 10 min each. This step was performed three times. Afterward, gel pieces were dried *in vacuo* and either stored at −80 °C or directly subjected to proteolytic digestion with trypsin (Promega, Mannheim, Germany) dissolved in 10 mM NH_4HCO_3 (pH 7.8) at a final concentration of 0.03 μg/μl. Protein spots were incubated overnight at 37 °C with 2 μl of trypsin solution and slight agitation. Proteolytic peptides were extracted twice with 10 μl of ACN and 5% formic acid mixed 1:1 (v/v); extracts were combined and ACN was removed *in vacuo*. For MS analysis, samples were acidified by addition of 5% formic acid to a final volume of 20 μl.

Mass Spectrometric Analysis and Protein Identification—Tryptic digests were analyzed by nano HPLC/ESI-MS/MS using a Dionex LC Packings system (Dionex LC Packings, Idstein, Germany) coupled to a QSTAR XL instrument (Applied Biosystems, Foster City, CA). Peptide mixtures were separated by online RP capillary HPLC as previously described by Schaefer *et al.* (33). The mass spectrometer was equipped with a nanoelectrospray ion source (SCIEX, Toronto, Ontario, Canada) and distal coated SilicaTips (FS360–20–10-D; New Objective, Woburn, MA). For external calibration of the QSTAR XL instrument in the enhanced product ion mode, reserpine (*m/z* 609.280; Agilent Technologies, Santa Clara, CA) and two of its fragments with *m/z* 174.100 and 195.065 were used. To guarantee high reproducibility of MS scans, calibration was routinely performed before and after the analysis of biological samples.

The general mass spectrometric parameters were set as follows: ion spray voltage (IS), 1800–2000 V; curtain gas (CUR), 10–14; gas 1, 0; declustering potential (DP), 50 V; focusing potential (FP), 220 V; declustering potential 2 (DP2), 15 V. In the Analyst QS 1.1 software (Applied Biosystems), the so-called "*I*nformation *D*ependent *A*cquisition" (IDA) method was chosen, which consists of a survey MS scan (*m/z* 400–1200) followed by sequential isolation and fragmentation of the three most intense peaks (enhanced product ion scans, *m/z* 100–2000). To obtain most informative peptide fragmentation spectra, only multiply charged peptide ions of interest were isolated in the quadrupole Q1 (set to low resolution) and subjected to collision-induced dissociation using nitrogen as collision gas. Furthermore, previously fragmented ions were dynamically excluded for the following 16 s. Depending on the mass-to-charge ratio of isolated peptides, collision energies for the fragmentation in the collision cell q2 were dynamically adjusted by the software (rolling collision energy).

Peaklists of MS/MS spectra were generated using the software Analyst QS 1.1 with default parameter settings. For peptide and protein identification, uninterpreted peptide ESI-MS/MS spectra were correlated with the *A. thaliana* EBI protein sequence database (ipi.ARATH.v3.17.fasta) containing 34,559 protein entries using SEQUEST (34, 35) (TurboSEQUEST v.27) after converting and exporting the raw data into the DTA format using the software tool wiff2dta (36). Species restriction to *A. thaliana* is justified by the fact that exclusively proteins from *A. thaliana* were analyzed. Database searches were performed with tryptic specificity allowing two missed cleavages and a mass tolerance of 0.2 Da for parent and fragment ions. Oxidation of methionine residues and formation of propionamide at cysteine residues were considered as variable modifications; no fixed modifications were included. Cut-off scores for accepting individual MS/MS spectra of doubly and triply charged peptides were 2.0 for the cross-correlation factor (Xcorr) and 0.1 for the delta normalized cross-correlation factor (35). Protein identification was based on at least two

distinct peptides. If a protein appeared under different names and accession numbers, the entry with the highest sequence coverage was selected. In the case that different protein isoforms were listed by SEQUEST, these entries were inspected manually and the presence of each protein isoform was confirmed by the identification of at least two unique peptides.

Relative Protein Quantification—For relative quantification of proteins showing differences in abundance based on fluorescence labeling and two-dimensional DIGE, the software DeCyder 6.0 was used. Criteria for significant protein regulation were as follows: Protein spots needed to 1) be present and analyzed in at least three gels per set of experiments and 2) show an average factor of ± 1.5 in both sets as well as 3) a Student's *t* test value of $p < 0.05$. For calculations of protein abundance ratios based on two-dimensional DIGE experiments, fluorescence intensities ("normalized spot volumes") for each channel of the different CyDyes were manually exported out of DeCyder and used for further processing. The fluorescence intensity of a ^{14}N-labeled protein was divided by the fluorescence intensity of the corresponding ^{15}N-labeled protein. Individual ratios obtained for proteins in reciprocally labeled sets of experiments were averaged and arithmetic mean values as well as the corresponding standard deviation were calculated for each protein per set.

For relative protein quantification based on metabolic ^{14}N/^{15}N labeling, the in-house developed software Peakardt was employed. For the export of peaklists from Analyst QS 1.1 for use in Peakardt, the threshold for "PeakFinding" in MS spectra and total ion chromatograms was set to 1.0%. Total ion chromatograms acquired in LC-MS/MS runs were divided into distinct time segments of 1 min; MS spectra within these intervals were summed up and used for further *in silico* processing. Abundance ratios of ^{14}N- (light) and ^{15}N-coded (heavy) peptides were calculated by dividing peak areas of light peptides by those of heavy peptides using the "FindPairs" algorithm of Peakardt. For relative quantification, the monoisotopic peak and generally two ^{13}C-isotope peaks of both light and heavy peptides as well as the first ^{14}N-satellite peak of the heavy peptide were taken into account. In case that peptide signal intensities were low, only one ^{13}C-isotope peak was considered. To improve the confidence of relative peptide quantification, an *in silico* digestion of identified proteins with trypsin was performed via Peakardt. Masses of theoretically determined ^{14}N/^{15}N-labeled peptides were then searched and matched with peptide masses present in the experimentally acquired mass spectra. Only peptide pairs that did not overlap with other peptides in their *m/z*-range were considered for further calculation of relative protein abundances. In addition, peptide pairs exceeding the 2.5-fold of the arithmetic mean determined by "FindPairs" were considered as outliers and removed. The determination of protein abundance ratios was based on at least two adequate peptide pairs. If not stated otherwise, a protein was considered as significantly regulated based on metabolic labeling and MS analysis when it 1) could be identified and quantified reliably in at least three gels per set of experiments and 2) showed an average regulation factor of ± 1.5 as well as 3) a Student's *t* test value of $p < 0.05$. The arithmetic mean of all peptides detected for each protein in all biological replicates per set, the deviation (in %), biological and technical variance, *p* value as well as the 95% confidence interval were calculated using the "ExperiAna" module of Peakardt.

Statistical Analyses—In the reverse labeling experiments described in this work, a protein with a distinct abundance ratio in one experiment (referred to as Set 1) is expected to have the reciprocal ratio in the experiment with reversed labeling (referred to as Set 2). Consequently, multiplication of both ratios is expected to result in a factor of 1. For the calculation of the standard deviation (S.D.) for this kind of analysis, the "propagation of error model" (37) was applied using the formula $(\Delta X/X)^2 = (\sigma_A/A)^2 + (\sigma_B/B)^2$, with $X = A \times B$, and *A* and *B* being the abundance ratio of a distinct spot or protein in Set 1 and Set 2; σ_A and σ_B denominate the respective S.D.; ΔX is the value "propagation of error" to be calculated as shown in Equation 1.

$$\Delta X = \sqrt{(\sigma_A/A)^2 + (\sigma_B/B)^2} \times X \qquad \text{(Eq.1)}$$

The same formula was used to determine the "propagation of error" when the average abundance ratios of proteins based on ^{15}N labeling were divided by the corresponding values obtained in DIGE experiments.

To detect outliers in data sets obtained in double and reverse labeling experiments, box plots were utilized (38, 39). They were plotted using the software R, version 2.5.1. With a box plot, the distribution characteristics of continuous data can be visualized. As with a histogram, accumulation points, distribution width, skew, and outliers can be described. The horizontal, bold line within the "box" represents the median and the small rectangle shows the arithmetic mean of the data set. The box itself contains the middle half of the data from first quartile to third quartile (interquartile distance). The vertical lines ending in horizontal lines above and below the box are called "whiskers." The horizontal lines lie on the last data point inside the 1.5-fold of the interquartile distance spanning from the box. Data points outside the whiskers are interpreted as "outliers" and drawn as filled circles.

RESULTS

^{14}N/^{15}N Labeling of Plants Grown on Solid Medium—So far, comparative proteomics studies on *A. thaliana* employing metabolic labeling have been performed using cultured suspension cells or plants grown in liquid cultures (13–18). However, in order to acquire biologically meaningful information on complex events related to, among others, plant development, metabolism, or responses to environmental influences, one should aim at growing plants under conditions that reflect their natural habitat as close as possible.

A major aim of the work presented here was to achieve complete metabolic labeling (*i.e.* ≥ 95% incorporation of stable isotopes) of entire *A. thaliana* plants grown on solid medium using ^{15}N. For this purpose, *A. thaliana* wt and *old1–1* mutant plants exhibiting advanced leaf senescence (20–22) were grown under standard conditions in a growth chamber as described in "Experimental Procedures." ^{15}N labeling of plants was performed by substituting KNO_3 and NH_4NO_3 in the medium with the respective ^{15}N-containing salts (>98% enriched in ^{15}N). To ensure efficient metabolic labeling, seeds of first-generation plants were harvested and sown once again onto solid, ^{15}N-containing growth medium. Control plants (^{14}N-labeled) were subjected to the same procedure. To study early leaf senescence, second generation plants were harvested after 16 days of growth. At this stage, incorporation of ^{15}N-isotopes into the proteins from both wt and mutant plants reached 95% (data not shown) as estimated using the software IsoPro 3.0.

Linearity of Relative Protein Quantification Based on ^{14}N/^{15}N Labeling—To evaluate the linearity of relative protein quantification based on ^{14}N/^{15}N labeling and MS, protein extracts from differentially labeled wt plants were mixed in distinct concentration ratios ranging from 1:5 (^{14}N:^{15}N) to 5:1. Follow-

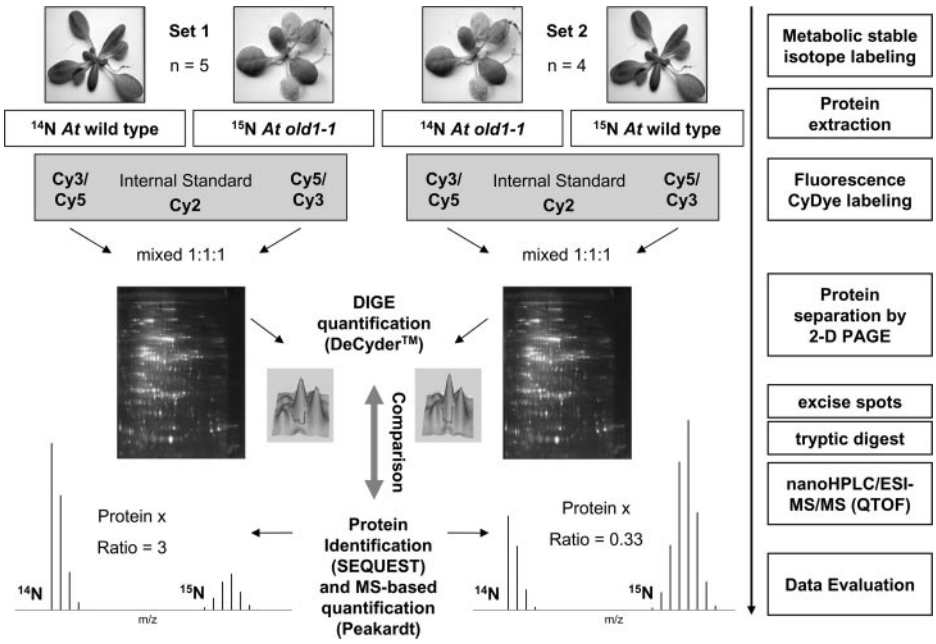

FIG. 1. **Experimental setup of the double and reverse labeling strategy for the relative quantitative analysis of *A. thaliana* wild type *versus old1–1* mutant plants**. *A. thaliana* (*At*) wt and *old1–1* mutant plants were grown in the presence of either ^{14}N-containing or >98% ^{15}N-enriched KNO_3 and NH_4NO_3 as sole nitrogen sources. In Set 1 ($n = 5$), wt plants were grown in ^{14}N, whereas *old1–1* mutant plants were labeled with ^{15}N; in Set 2 ($n = 4$), labeling was reversed. Following harvesting and protein extraction, protein samples and an internal standard were differentially labeled with CyDyes (Cy3, Cy5, or Cy2) and mixed in equal ratios; proteins were separated by two-dimensional PAGE. Relative protein quantification was performed based on 1) the fluorescence intensities of protein spots using DeCyder and 2) peak areas of ^{14}N/^{15}N-labeled peptides using the software Peakardt. For protein identification by database searches using SEQUEST, spots of interest were excised, subjected to in-gel tryptic digestion, and analyzed by nano HPLC/ESI-MS/MS.

ing two-dimensional PAGE and visualization by colloidal Coomassie Blue, 18 corresponding protein spots covering a wide range of molecular weight and pI were excised from each gel and subjected to nano HPLC/ESI-MS/MS analysis. Since we observed co-elution of ^{14}N/^{15}N-labeled peptides from the RP column (data not shown), differences in the chromatographic behavior of peptide pairs did not need to be considered. MS-based relative protein quantification in the entire study was performed by calculating peak ratios of ^{14}N/^{15}N-labeled peptides based on peak areas using the in-house developed software Peakardt (see "Experimental Procedures"). Protein abundance ratios were calculated based on 4.5 peptide pairs on average. The average protein concentration ratios were in good accordance with the theoretical ratios ranging from 1:5 to 5:1 as reflected by the correlation coefficient of 0.9965 (supplemental Fig. 1). Relative errors between theoretical and experimental values were in the range of 7% for the 1:1 and 21% for the 1:5 ratios.

Design of Double and Reverse Labeling Strategy—For assessment whether metabolic labeling is applicable to address biological questions in plant proteomics, a double and reverse labeling strategy concomitantly employing DIGE and ^{14}N/^{15}N labeling was designed. Reverse labeling experiments were carried out to reveal potential inconsistencies in protein quantification caused by the labeling technique employed. Moreover, reverse ^{14}N/^{15}N labeling allows the detection of possible adverse effects on an organism's development and protein expression that may occur during the process of differential labeling, including heavy isotope effects (11, 16). An additional benefit of reverse ^{15}N labeling is the improved ability to detect and quantify strongly regulated proteins by MS (40). Double labeling provides a reciprocal control for both strategies and allows to evaluate the consistency of the results obtained by the two different techniques for protein quantification (23).

In this work, two sets of experiments were carried out (Fig. 1). In the first set, referred to as Set 1, wt plants were grown in a medium containing ^{14}N while *old1–1* mutant plants were labeled with ^{15}N. In the second set (Set 2), labeling was reversed. To take into account biological variations and to gain statistically significant data on differences in protein abundance, five (Set 1) and four (Set 2) independent experiments were performed. After harvesting the plants and protein extraction, proteins were differentially labeled with CyDyes as follows: In three of five replicates in Set 1, proteins derived from wt plants were labeled with Cy5 while proteins from mutant plants were labeled with Cy3. In the remaining two replicates, fluorescent labeling was reversed. The same labeling strategy was applied to the experiments of Set 2, with two replicates each. This color switch is routinely used to eliminate effects of a possible preferential affinity of different fluorescent dyes to proteins of one of the samples analyzed (41).

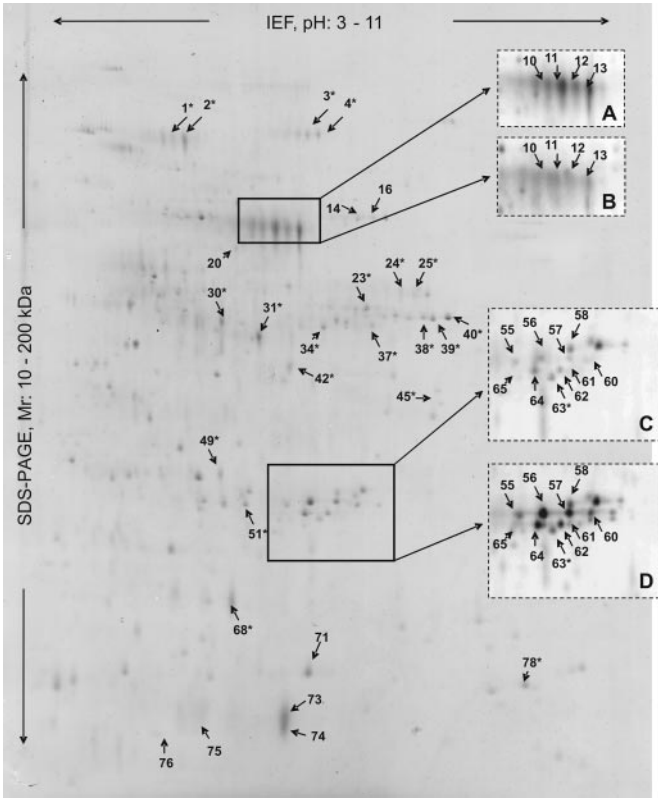

FIG. 2. **Distribution of protein spots on a representative two-dimensional DIGE gel poststained with colloidal Coomassie.** Proteins derived from wt plants were labeled with Cy3 and mixed with Cy5-labeled proteins from *old1–1* mutant plants as well as an internal standard labeled with Cy2 in equal ratios. Proteins were separated by two-dimensional PAGE and subsequently visualized with colloidal Coomassie Brilliant Blue. Numbers indicate regulated (*arrow* only) and nonregulated spots (*arrows* and *) as determined by DIGE that were further subjected to MS analysis for both protein identification and quantification. *Squares* highlight areas with protein spots exhibiting major differences in protein abundance. *A–D*, corresponding images of Cy3-labeled wt proteins (*A* and *C*) and Cy5-labeled *old1–1* mutant proteins (*B* and *D*). Images were converted from fluorescence into false color images using the software ImageQuant 5.2.

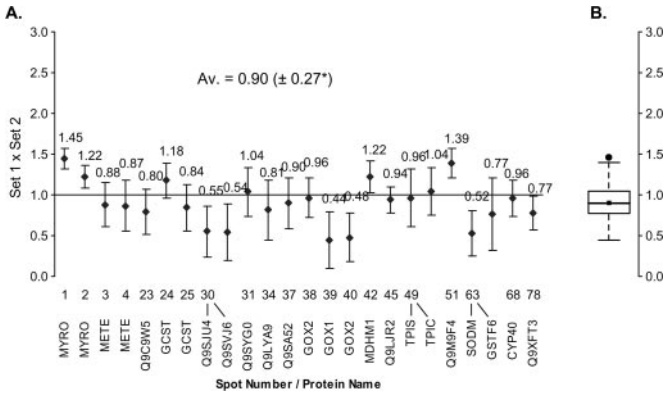

FIG. 3. **Evaluation of metabolic labeling of *A. thaliana* plants with respect to possible artificial effects of ^{15}N-incorporation on protein abundance**. *A*, following MS-based relative protein quantification, the abundance ratios calculated for proteins in Set 1 (^{14}N-labeled wt *versus* ^{15}N-labeled *old1–1*) were multiplied with the ratios of the corresponding protein in Set 2 (^{14}N-labeled *old1–1 versus* ^{15}N-labeled wt). This analysis was based on protein spots that did not show differences in fluorescent intensities. *Numbers* correspond to *spot numbers* in Fig. 2; abbreviations of protein names correspond to the UniProtKB/Swiss-Prot database. More detailed information about proteins, including full protein name, IPI accession number, peptide abundance ratios, and sequence coverage, are provided in supplemental Tables S2, S5, and S6. *B*, *box plot* based on the mean values of the data illustrated in *A*. *Deviation expressed as root mean squared error.

However, no such effects were observed in this study (data not shown). Differentially labeled protein samples and an aliquot of the corresponding internal standard were combined in a 1:1:1 ratio and subjected to two-dimensional PAGE. Following image analysis using the software DeCyder, selected protein spots were analyzed by nano HPLC/ESI-MS/MS on a QTOF instrument. Fig. 2 shows the overall distribution of protein spots on a representative two-dimensional DIGE gel post-stained with colloidal Coomassie Brilliant Blue. Numbers indicate both regulated (marked with an arrow only) and nonregulated spots (marked with arrow and asterisk) reported in this work (supplemental Tables S1 and S2).

^{15}N Labeling Did Not Cause Adverse Effects on Plants—To address the question whether ^{15}N labeling of *A. thaliana* plants resulted in artificial changes in protein abundance, 21 protein spots that did not show significant regulation based on DIGE in both Set 1 and Set 2 were analyzed by MS. A total of 20 different proteins were identified. In three spots, two distinct proteins were present (supplemental Table S2). Following MS-based protein identification and relative quantification, protein abundance ratios calculated for each protein in Set 1 were multiplied with the ratio of the corresponding protein in Set 2 (Fig. 3*A*). This resulted in an average value of 0.90 (± 0.27), indicating good correlation between both data sets. Calculations of this kind were based on the arithmetic mean of the sum of peptides detected for a distinct protein in all replicates. Standard deviations were determined according to the "propagation of error model" (37) as described under "Experimental Procedures." Average values for biological and technical variance of this data were 70.7% and 29.3% in Set 1 and 79.3% and 20.3% in Set 2 (for values of individual proteins, see supplemental Tables S5 and S6). As visualized by the box plot in Fig. 3*B*, subsequent statistical analysis uncovered the presence of one outlier in this data set. Interestingly, closer inspection of the values determined for individual proteins based on ^{14}N/^{15}N labeling revealed that one of the proteins identified in spot number 63, a GST isoform, showed significant differences in abundance ratios both in Set 1 and in Set 2, suggesting that this protein in fact is significantly regulated.

Differentially Regulated Proteins Detected in A. thaliana old1–1 *Plants*—Of ~900 protein spots that were matched by the DeCyder software in all gels, 21 spots consistently showed differences in fluorescent intensities between *A. thali-*

TABLE I

Proteins found to be significantly regulated in A. thaliana old1–1 *mutant plants*

Proteins showed significant differences in abundance in at least three independent replicates in Set 1 and Set 2 based on DIGE and ^{14}N/^{15}N-labeling combined with MS. Protein names, IPI accession numbers, abbreviated protein names according to the UniProtKB/Swiss-Prot database, spot numbers corresponding to numbers in Figure 2, average abundance ratios for each protein as well as the corresponding regulation factors are provided. For the GST isoforms, the terms according to the current nomenclature for plant GSTs (42, 43) are indicated as well. RuBisCO, ribulose 1,5-bisphosphate carboxylase/oxygenase; CV, coefficient of variation; S.D., standard deviation.

Protein (IPI accession)	Abbreviated protein name	Spot	Set	Metabolic labeling		DIGE	
				Average abundance ratio (± S.D.)	Regulation factor (± CV in %)	Average abundance ratio (± S.D.)	Regulation factor (± CV in %)
RuBisCO large subunit (IPI00535114.1)	RBL	10	1	2.28 (± 0.53)	−2.3 (± 23.2)	1.69 (± 0.43)	−1.7 (± 25.4)
			2	0.48 (± 0.14)	−2.1 (± 29.2)	0.59 (± 0.15)	−1.7 (± 25.4)
		11	1	2.00 (± 0.49)	−2.0 (± 24.5)	1.78 (± 0.40)	−1.8 (± 22.5)
			2	0.51 (± 0.10)	−2.0 (± 19.6)	0.57 (± 0.11)	−1.8 (± 19.3)
		12	1	2.24 (± 0.58)	−2.2 (± 25.9)	1.61 (± 0.50)	−1.6 (± 31.1)
			2	0.42 (± 0.14)	−2.4 (± 33.3)	0.58 (± 0.15)	−1.7 (± 25.9)
		13	1	2.07 (± 0.44)	−2.1 (± 21.3)	1.68 (± 0.52)	−1.7 (± 31.0)
			2	0.57 (± 0.10)	−1.8 (± 17.5)	0.54 (± 0.03)	−1.9 (± 5.6)
RuBisCO small subunit 1A (IPI00539020.1)	RBS1A	74	1	1.73 (± 0.44)	−1.7 (± 25.4)	1.61 (± 0.48)	−1.6 (± 29.8)
			2	0.45 (± 0.08)	−2.2 (± 17.8)	0.54 (± 0.12)	−1.9 (± 22.2)
		76	1	1.75 (± 0.11)	−1.8 (± 6.3)	1.75 (± 0.41)	−1.8 (± 23.4)
			2	0.45 (± 0.08)	−2.2 (± 17.8)	0.65 (± 0.14)	−1.5 (± 21.5)
RuBisCO small subunit 1B (IPI00521186.1)	RBS1B	75	1	1.59 (± 0.35)	−1.6 (± 22.0)	1.54 (± 0.26)	−1.5 (± 16.9)
			2	0.50 (± 0.13)	−2.0 (± 26.0)	0.55 (± 0.24)	−1.8 (± 43.6)
RuBisCO small subunit 2B (IPI00523477.1)	RBS2B	73	1	1.75 (± 0.47)	−1.8 (± 26.9)	1.76 (± 0.28)	−1.8 (± 15.9)
			2	0.37 (± 0.06)	−2.7 (± 16.2)	0.54 (± 0.12)	−1.9 (± 22.2)
Major latex protein-related (IPI00531983.1)	Q9SUR0	71	1	3.00 (± 0.43)	−3.0 (± 14.3)	2.16 (± 0.57)	−2.2 (± 26.4)
			2	0.36 (± 0.06)	−2.8 (± 16.7)	0.49 (± 0.10)	−2.0 (± 20.4)
Serine hydroxymethyltransferase, mitochondrial precursor (IPI00525727.1)	GLYM	14	1	0.62 (± 0.07)	1.6 (± 11.3)	0.61 (± 0.12)	1.6 (± 19.7)
			2	1.29 (± 0.68)	1.3 (± 52.7)	1.54 (± 0.40)	1.5 (± 26.0)
		16	1	0.59 (± 0.15)	1.7 (± 25.4)	0.57 (± 0.07)	1.8 (± 12.3)
			2	1.08 (± 0.34)	1.1 (± 31.5)	1.55 (± 0.23)	1.6 (± 14.8)
Enolase (IPI00526310.1)	ENO	20	1	0.66 (± 0.11)	1.5 (± 16.7)	0.63 (± 0.13)	1.6 (± 20.6)
			2	2.60 (± 0.57)	2.6 (± 21.9)	1.80 (± 0.36)	1.8 (± 20.0)
Quinone reductase (IPI00529112.1)	Q9LSQ5	55	1	0.57 (± 0.11)	1.8 (± 19.3)	0.24 (± 0.10)	4.2 (± 41.7)
			2	2.43 (± 0.67)	2.4 (± 27.6)	3.25 (± 1.11)	3.3 (± 34.2)
Glutathione S-transferase PM24, *At*GSTF2 (IPI00535149.2)	GSTF4	56	1	0.09 (± 0.03)	11.1 (± 33.3)	0.13 (± 0.02)	7.7 (± 15.4)
			2	16.64 (± 3.64)	16.6 (± 21.9)	7.51 (± 2.41)	7.5 (± 32.1)
		57	1	0.07 (± 0.02)	14.3 (± 28.6)	0.13 (± 0.06)	7.7 (± 46.2)
			2	18.33 (± 4.07)	18.3 (± 22.2)	11.15 (± 4.59)	11.2 (± 41.2)
		58	1	0.05 (± 0.02)	20.0 (± 40.0)	0.60 (± 0.19)	1.7 (± 31.7)
			2	17.59 (± 5.10)	17.6 (± 29.0)	3.07 (± 0.90)	3.1 (± 29.0)
		61	1	0.05 (± 0.02)	20.0 (± 40.0)	0.20 (± 0.07)	5.0 (± 35.0)
			2	22.25 (± 7.70)	22.3 (± 34.6)	6.58 (± 3.92)	6.6 (± 59.6)
Glutathione S-transferase *At*GSTF9 (IPI00538125.1)	O80852	58	1	0.53 (± 0.11)	1.9 (± 20.8)	0.60 (± 0.19)	1.7 (± 31.7)
			2	2.26 (± 0.81)	2.3 (± 35.8)	3.07 (± 0.90)	3.1 (± 29.0)
Glutathione S-transferase 11 *At*GSTF7 (IPI00530258.1)	GST11	60	1	0.02 (± 0.01)	50.0 (± 50.0)	0.16 (± 0.03)	6.3 (± 18.8)
			2	36.03 (± 5.44)	36.0 (± 15.1)	7.35 (± 1.29)	7.4 (± 17.6)
Glutathione S-transferase 1 *At*GSTF6 (IPI00548409.1)	GSTF1	62	1	0.22 (± 0.05)	4.5 (± 22.7)	0.32 (± 0.11)	3.1 (± 34.4)
			2	6.12 (± 2.10)	6.1 (± 34.3)	3.71 (± 1.54)	3.7 (± 41.5)
		64	1	0.17 (± 0.04)	5.9 (± 23.5)	0.23 (± 0.03)	4.3 (± 13.0)
			2	8.14 (± 3.89)	8.1 (± 47.8)	4.55 (± 0.44)	4.6 (± 9.7)
		65	1	0.17 (± 0.06)	5.9 (± 35.3)	0.25 (± 0.06)	4.0 (± 24.0)
			2	9.69 (± 4.41)	9.7 (± 45.5)	6.60 (± 1.43)	6.6 (± 21.7)
Glutathione S-transferase 6[a] *At*GSTF8 (IPI00536062.1)	GSTF6	63	1	0.42 (± 0.19)	2.4 (± 45.2)	0.75 (± 0.29)	1.3 (± 38.7)
			2	1.83 (± 0.68)	1.8 (± 37.2)	1.50 (± 0.31)	1.5 (± 20.7)

[a]This protein did not meet the criteria for significant regulation based on DIGE.

ana wt and mutant plants in both sets of experiments reciprocally labeled with ^{14}N/^{15}N. MS analyses of these spots (marked in Fig. 2) resulted in the identification of 12 distinct proteins or protein subunits. In one of the spots (number 58), two different isoforms belonging to the GST superfamily could reliably be identified. Table I lists all proteins found to be significantly up- or down-regulated in this study, including the GST isoform present in spot number 63. In addition, the table provides information on the average protein abundance ratios determined based on both peak areas of ^{14}N/^{15}N-labeled peptides and fluorescence intensities as well as the corresponding regulation factors. For the GST isoforms, the de-

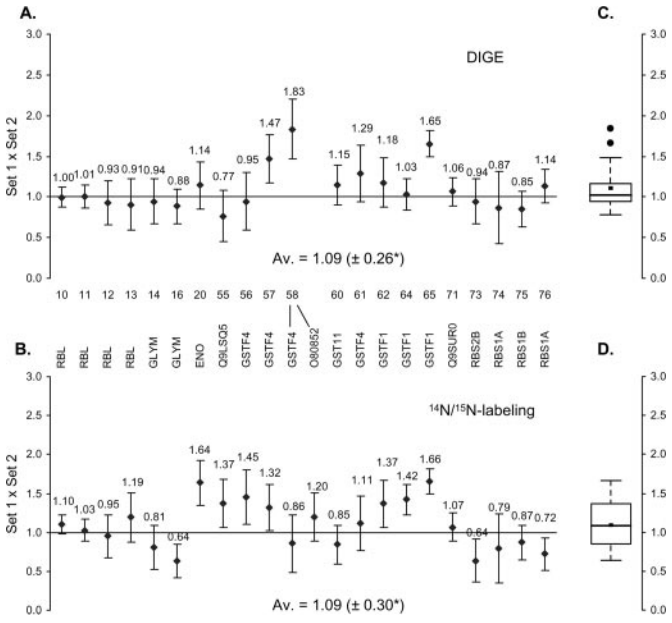

FIG. 4. **Consistency of abundance ratios of ^{14}N/^{15}N-labeled proteins from reciprocally labeled *A. thaliana* wild type and mutant plants**. Abundance ratios calculated for proteins in Set 1 (^{14}N-labeled wt *versus* ^{15}N-labeled *old1–1*) were multiplied with the ratios of the corresponding proteins in Set 2 (^{14}N-labeled *old1–1 versus* ^{15}N-labeled wt); relative quantification of proteins showing significant regulation as revealed by DIGE was either based on fluorescent intensities (*A*) or on metabolic stable isotope labeling and MS (*B*). *Numbers* correspond to *spot numbers* in Fig. 2; abbreviations of protein names correspond to the UniProtKB/Swiss-Prot database. More detailed information about identification and quantification of proteins are provided in supplemental Tables S1, S3, and S4. *C* and *D*, *box plots* relying on the mean values of the data plotted in part *A* and part *B*, respectively. Deviation expressed as root mean squared error.

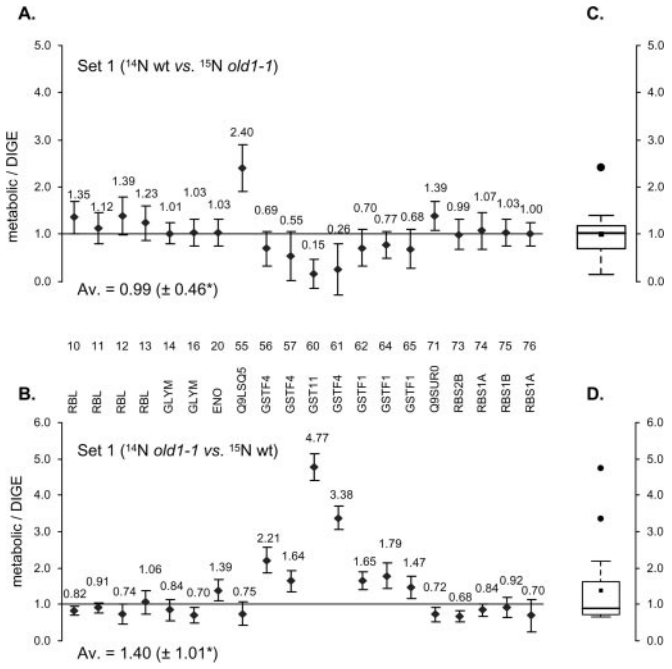

FIG. 5. **Comparison of relative protein quantification based on DIGE *versus* ^{14}N/^{15}N labeling combined with MS.** Abundance ratios determined by quantitative MS were divided by the corresponding ratios obtained by DIGE for proteins in Set 1 (*A*) and in Set 2 (*B*). For spot numbers see Fig. 2; protein names are abbreviated according to the UniProtKB/Swiss-Prot database. *C* and *D*, Box plots based on the mean values of the data plotted in part *A* and part *B*, respectively. Deviation expressed as root mean squared error.

nominations according to the current nomenclature for plant GSTs (42, 43), which will be used in the following, are given as well. *Squares* in Fig. 2 highlight areas showing major differences in protein abundance as revealed by two-dimensional DIGE analysis. Insets show corresponding images of Cy3-labeled wt proteins (Figs. 2*A* and *C*) and Cy5-labeled *old1–1* mutant proteins (Figs. 2*B* and *D*). The protein underlying all four spots in Figs. 2*A* and *B*, identified as the large subunit of ribulose 1,5-bisphosphate carboxylase/oxygenase (RuBisCO), was down-regulated in mutant plants. Further proteins with decreased abundance in *old1–1* plants were RuBisCO small subunits 1A, 1B, and 2B as well as a protein with similarity to major latex protein. Densitometric intensities of spots marked in Figs. 2*C* and *D* indicate significant up-regulation of the respective proteins in *old1–1* mutant compared with wt plants. These proteins predominantly belonged to the family of GSTs. In addition to *At*GSTF2, *At*GSTF6, *At*GSTF7, *At*GSTF8 (identified in spot number 63), and *At*GSTF9, the proteins serine hydroxymethyltransferase mitochondrial precursor, enolase as well as quinone reductase showed higher abundances in the *old1–1* mutant.

Comparison of Protein Quantification via Two-dimensional DIGE and ^{14}N/^{15}N Labeling Combined with MS—The consistency of the results obtained for reciprocally ^{14}N/^{15}N-labeled proteins based on (I) fluorescence scanning and (II) peptide MS analysis was validated by multiplying the average abundance ratios of corresponding protein spots/proteins of Set 1 and Set 2. On average, the products of protein abundance ratios based on DIGE (Fig. 4*A*) were 1.09 (± 0.26) and 1.09 (± 0.30) based on ^{14}N/^{15}N labeling (Fig. 4*B*), which indicates high consistency of the reverse labeling experiment. The averages of biological and technical variance for the MS-based data were consistent with those observed for the nonregulated proteins (80.8% and 19.2% in Set 1 and 76.7% and 23.3% in Set 2; for values of individual proteins, see supplemental Tables S3 and S4). The box plot for the data obtained using DIGE (Fig. 4*C*) indicates the presence of two outliers. These are spot number 58, corresponding to two members of the GST family, and spot number 65 (*At*GSTF6) with values of 1.83 and 1.65, respectively. No outliers were detected for the data based on ^{15}N labeling (Fig. 4*D*).

To evaluate the comparability of relative protein quantification based on DIGE and ^{14}N/^{15}N labeling, corresponding average protein abundance ratios were divided. This was performed for each spot in Set 1 and Set 2, except for spot number 58, as this spot contained two different proteins. For Set 1 (Fig. 5*A*), an average value of 0.99 (± 0.46) with individ-

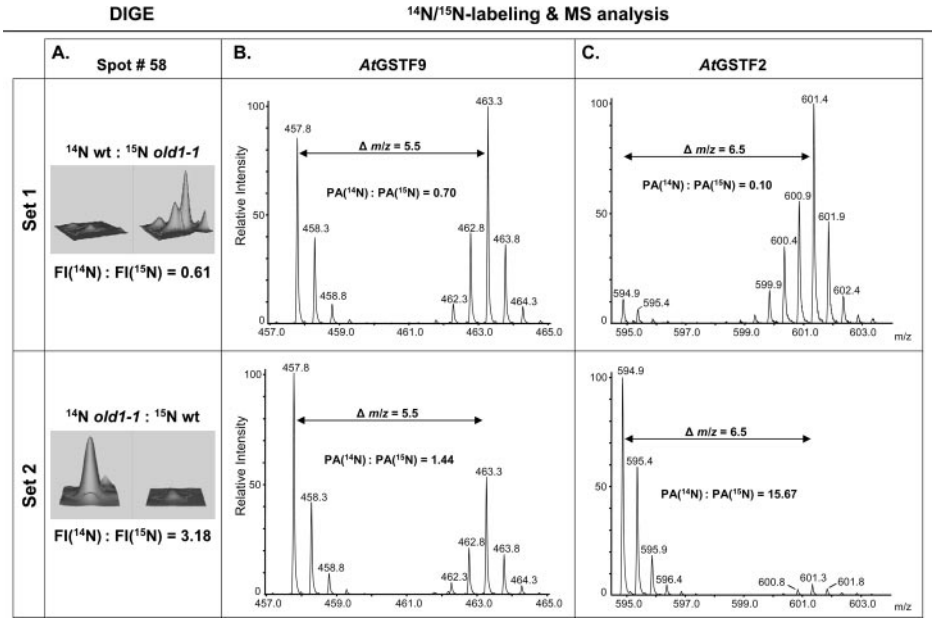

FIG. 6. **Example of relative protein quantification using DIGE and ^{14}N/^{15}N labeling combined with MS.** *A*, three-dimensional views of the fluorescence intensities (FI) of spot number 58 in Set 1 (*top*) and Set 2 (*bottom*) extracted from the DeCyder software. For relative quantification, the FI of the ^{14}N-labeled proteins (FI^{14}N) was divided by the FI of the ^{15}N-labeled proteins (FI^{15}N). *B* and *C*, Representative sections of mass spectra showing tryptic ^{14}N/^{15}N-labeled peptides derived from *At*GSTF9 (*B*; SQGPDLLGK) and *At*GSTF2 (*C*; VNEWVAEITK) identified in spot number 58 for Set 1 (*top*) and Set 2 (*bottom*). Protein abundance ratios were determined by dividing the peak area (PA) of the ^{14}N-labeled peptide by the PA of the ^{15}N-labeled peptide. Δ*m/z*, shift in *m/z* resulting from the incorporation of ^{15}N into the peptides; *wt*, wild type.

ual values between 0.15 and 2.40 was calculated while the average value for Set 2 (Fig. 5*B*) was determined to be 1.40 (± 1.01) with individual values ranging from 0.68 to 4.77. Box plots revealed that the data in Set 1 show a skew to the lower quartile (Fig. 5*C*); in Set 2, the data are skewed to the upper quartile (Fig. 5*D*). One outlier was detected in Set 1, quinone reductase in spot number 55. In Set 2, two outliers were present, namely *At*GSTF7 in spot number 60 and *At*GSTF2 in spot number 61.

Fig. 6 shows a comparison of relative protein quantification based on fluorescent labeling and densitometry (Fig. 6*A*) and MS analysis of ^{14}N/^{15}N-labeled peptide pairs (Figs. 6*B* and *C*). Fig. 6*A* depicts 3-D views of the fluorescence intensities (FI) of both proteins, namely *At*GSTF9 and *At*GSTF2, identified in spot number 58 in Set 1 (*top*) and Set 2 (*bottom*). Data from individual DIGE gels were extracted from the DeCyder software. For Set 1, the FI of this spot from ^{14}N-labeled wt proteins was divided by the FI of the ^{15}N-labeled counterparts from the *old1–1* mutant, yielding a ratio of 0.61. For Set 2, a ratio of 3.18 was obtained. These abundance ratios, however, do not reflect the ratios of the two individual proteins present in this spot. Figs. 6*B* and *C* show mass spectra of the ^{14}N/^{15}N-labeled peptide SQGPDLLGK derived from *At*GSTF9 and VNEWVAEITK from *At*GSTF2, respectively. The doubly charged peptide SQGPDLLGK ($C_{39}H_{67}N_{11}O_{14}$) is detected at *m/z* 457.8, its heavy counterpart at *m/z* 463.3 (Fig. 6*B*). Accordingly, for the doubly charged peptide VNEWVAEITK ($C_{54}H_{85}N_{13}O_{17}$) of *At*GSTF2 a mass shift of 6.5 Da is observed due to ^{15}N labeling (Fig. 6*C*). The ^{14}N/^{15}N-labeled tryptic peptides SQGPDLLGK from *At*GSTF9 exhibited an abundance ratio of 0.70 in Set 1 and 1.44 in Set 2 (Fig. 6*B*, *top* and *bottom*). Note that the average factors for this protein across all replicates were 0.53 in Set 1 and 2.26 in Set 2 indicating a significant 2-fold up-regulation of *At*GSTF9 in *old1–1*. Relative abundance ratios for the peptide VNEWVAEITK derived from *At*GSTF2 (Fig. 6*C*) were 0.10 in Set 1 and 15.67 in Set 2. The overall ratios of this protein across all replicates were 0.05 in Set 1 and 17.18 in Set 2. This corresponds to a regulation factor of approximately +20 for the *At*GSTF2 isoform, which is 10-fold higher than that of *At*GSTF9 present in the same spot. In contrast to MS-based quantification, DIGE does not allow for calculating individual values for each protein. The factors for both proteins determined based on DIGE were +1.7 in Set 1 and +3.1 in Set 2 (Table I).

DISCUSSION

To analyze changes in protein abundance occurring during early leaf senescence, we developed a comprehensive quantitative proteomics strategy comprising differential labeling of proteins from *A. thaliana* wt and *old1–1* mutant plants using CyDyes and ^{14}N/^{15}N-isotopes followed by MS (Fig. 1). We used second-generation plants harvested after 16 days of growth. This time point was chosen because our focus was to identify alterations in protein abundance during early leaf senescence, *i.e.* the stage before visible symptoms of leaf senescence occur. In *old1–1* mutants grown on solid medium, visible yellowing was not observed before day 17 (data not shown). We successfully demonstrated that full labeling with ^{15}N, which has recently been reported for *A. thaliana* suspension cultures or plants grown in liquid culture (14–18), is equally feasible for entire *A. thaliana* plants grown on solid medium representing more natural growth conditions for this species. Following a labeling scheme spanning two generations, incorporation of ^{15}N into the proteins of wt and *old1–1* mutant plants amounted to 95%. Using distinct mixtures of protein extracts from ^{14}N/^{15}N-labeled wt plants, we evaluated

the accuracy of MS-based relative protein quantification in the range of 1:5 to 5:1 and found a high correlation ($R^2 = 0.9965$) between experimental and theoretical values (supplemental Fig. 1). This is in accordance with findings reported by Huttlin *et al.* showing that quantification is accurate for ratios between 1:12 and 12:1 (16). We observed relative errors between 7% for the 1:1 ratio and up to 21% for higher mixing ratios, which is in the range of those found in previous studies (15, 44).

The simultaneous use of DIGE and ^{14}N/^{15}N labeling combined with MS provided us with two independent approaches, which allowed us not only to assess the applicability of metabolic ^{15}N labeling for quantitative plant proteomics but also to directly compare the capacity of both methods. Reversed ^{14}N/^{15}N labeling enabled us to demonstrate that the labeling did not have any side effects on protein expression and development of *A. thaliana* plants. For this, we analyzed 21 protein spots showing no regulation based on DIGE and performed at least four independent experiments per set to gain statistically sound data. Multiplication of abundance ratios based on ^{14}N/^{15}N-labeled peptides calculated for proteins in Set 1 and Set 2 yielded an average value of 0.90 (± 0.27) (Fig. 3*A*), indicating high consistency between both data sets. Overall, MS-based quantification results confirmed the DIGE findings, *i.e.* that the proteins underlying the spots do not exhibit differences in abundance between wt and mutant plants. However, we could identify one protein, *At*GSTF8, which consistently exhibited a regulation factor of approximately +2 in both sets that could not be detected by DIGE.

Our double and reverse labeling strategy resulted in the determination of 13 proteins and protein subunits that showed significant regulation in the *old1–1* mutant compared with *Arabidopsis* wt plants. All proteins showed consistent regulation in both sets based on either DIGE (Fig. 4*A*) or ^{14}N/^{15}N labeling and MS (Fig. 4*B*). In addition, average values of 1.09 (± 0.26) for DIGE and 1.09 (± 0.30) for quantitative MS across all proteins indicate a very good correlation between Set 1 and Set 2 for both quantification strategies. Statistical analyses did not reveal any outliers in the data set based on ^{14}N/^{15}N labeling (Fig. 4*D*), whereas two outliers were detected in the data set derived from DIGE (Fig. 4*C*). These were spots number 58 and 65 with average values of 1.83 and 1.65. Both spots exhibited diffuse spot borders, which may have introduced small errors leading to a poor correlation between both sets of experiments.

To assess the comparability of DIGE and ^{14}N/^{15}N labeling combined with MS for relative protein quantification, we divided the average abundance ratios of proteins determined by either method (note that only single protein-containing spots showing significant regulation were considered). The average values across all 20 protein spots were 0.99 (± 0.46) for Set 1 (Fig. 5*A*) and 1.40 (± 1.01) for Set 2 (Fig. 5*B*), indicating high consistency between both quantification methods. Statistical analyses revealed the presence of one outlier in Set 1, the protein quinone reductase in spot number 55, and two outliers in Set 2, namely *At*GSTF7 in spot number 60 and *At*GSTF2 in spot number 61. Both GST isoforms were consistently found to be highly regulated in all experiments (Table I). The average values determined for the individual proteins based on ^{14}N/^{15}N labeling, however, were 3- (*At*GSTF2 in Set 2) to 8-fold (*At*GSTF7 in Set 1) higher than those obtained by DIGE. This drift is more pronounced in Set 1, which is a reasonable explanation why these GSTs were classified as outliers in this data set. Interestingly, the tendency toward the determination of considerably higher regulation factors following MS-based quantification is true for all proteins in our study exhibiting regulation beyond the factor of ± 3 (Table I). Consequently, the correlation between DIGE and MS-based quantification is lower for proteins with regulation factors exceeding −3 and +3. Box plots visualize this observation by showing a skew to the lower quartile for Set 1 (Fig. 5*C*) and a skew to the upper quartile for Set 2 (Fig. 5*D*). Our results correspond to observations made by Kolkman *et al.* who evaluated the comparability of DIGE and ^{15}N labeling combined with MS in a quantitative proteomic study of different yeast strains (23). They found a good correlation between both quantification techniques as long as the protein concentration ratios were within the range of −3 to +3, too. Beyond these margins, however, they also observed that MS provided higher values for protein concentration ratios. According to Huttlin *et al.* (16), MS-based quantification based on full metabolic labeling results in accurate values for regulation factors of ±12. To our knowledge, analogous data for DIGE experiments are not available. At present, it is therefore not possible to assess which quantification technique is more reliable and better suited for the determination of abundance ratios of proteins exhibiting rather extreme changes in abundance. Further studies are necessary to clarify this question. A promising approach to address this issue is the use of partial metabolic labeling. In a comparative study of full (> 98% ^{15}N) *versus* partial metabolic labeling (5–6% ^{15}N) of *A. thaliana* plants, Huttlin *et al.* demonstrated that the latter is superior for the analysis of proteins exhibiting large differences in protein abundance (16).

Fig. 6 demonstrates basic features of DIGE (Fig. 6*A*) and MS for relative protein quantification (Figs. 6*B* and *C*). While differences in protein abundance are typically immediately apparent following fluorescence image analysis and usually only regulated protein spots are subsequently identified by MS, stable isotope labeling combined with MS enables the global identification and quantification of proteins in the same experiment. Moreover, a general advantage of metabolic labeling and MS is the capability to quantify accurately different proteins comigrating during electrophoresis as illustrated for the proteins *At*GSTF9 and *At*GSTF2 both present in spot number 58 (Figs. 6*B* and *C*). MS-based quantification revealed that the two GST isoforms exhibited striking differences in abundance ratios; *At*GSTF9 was ~2-fold up-regulated in *old1–1* mutant plants while *At*GSTF2 exhibited a

regulation factor of roughly +20. Based on DIGE, however, only one value was obtained for both proteins, *i.e.* +1.7 in Set 1 and +3.1 in Set 2 (Table I).

We reliably identified five distinct proteins or protein subunits that were significantly down-regulated in old*1–1* mutant plants, RuBisCO large subunit, RuBisCO small subunits 1A, 1B, and 2B as well as a protein related to major latex protein. RuBisCO is the key enzyme of the photosynthetic CO_2 fixation and consists of eight large and eight small subunits. It catalyzes the carboxylation of D-ribulose 1,5-bisphosphate, the primary event in carbon dioxide fixation, as well as the oxidative fragmentation of the pentose substrate. Reduction in RuBisCO levels has been associated with senescence and its degradation may be triggered by reactive oxygen species (reviewed in (45)), such as ozone. In agreement with this idea, our results consistently showed an ~2-fold decrease of all RuBisCO subunits at a developmental stage (16 days) before symptoms of leaf senescence are visible. Against the background of extensive changes in the metabolism of senescing leaves for the purposes of nutrient retrieval, reduction in RuBisCO levels is a necessary consequence. Indeed, it has been reported that the earliest structural hallmark of leaf senescence is the disintegration of chloroplasts, which is accompanied by, among others, the progressive loss of RuBisCO on the biochemical level (19). A further protein with a 2- to 3-fold lower abundance in the *old1–1* mutant was a protein related to major latex protein (MLP). MLPs were first isolated from the latex of opium poppy and have since been found to be present in a number of other plants and tissues, including *Arabidopsis* (46, 47). The general function of this protein family is still unknown; follow-up studies are necessary to clarify whether MLPs are of relevance for early leaf senescence.

Most of the proteins found to be highly up-regulated in *old1–1* mutant plants belong to the large family of glutathione S-transferases, which are generally known as detoxifying enzymes. Among these GSTs (*At*GSTF2, *At*GSTF6, *At*GSTF7, *At*GSTF8, *At*GSTF9), *At*GSTF7 showed particularly high regulation factors of up to +36 (± 15.1%) in Set 2 and +50 (± 50%) in Set 1 (calculated based on ^{14}N/^{15}N labeling and MS analysis; Table I). *At*GSTF2, which was identified in four distinct spots, was ~10- to 20-fold up-regulated while the regulation factors of the other GSTs were in the range of +2 to +10. In plants, GSTs are mainly cytosolic and homodimeric or heterodimeric proteins that were shown to be involved in stress tolerance as well as in the detoxification of herbicides, organic pollutants, and natural toxins (48). Plant GSTs are currently classified into six distinct classes (49), two of which, phi and tau, are plant-specific (50). These are typically up-regulated in response to biotic stress including osmotic stress, extreme temperatures, and infection or treatments that evoke plant defense reactions (24). There are reports about increased expression of several GSTs during leaf senescence (51–53). Interestingly, the isoforms found to be up-regulated in the *A. thaliana old1–1* mutant in our study are all assigned to the phi class. Among those, only *At*GSTF8 has been linked to leaf senescence yet (51). In general, the expression of GSTs of class phi was reported to be predominantly induced by oxidative and pathogen stress (54). It is of interest to note that investigations of the transcriptome of a further *A. thaliana* mutant also exhibiting an early leaf senescence phenotype, *constitutive expressor of pathogenesis-related genes 5* (*cpr5*), which is allelic to *old1–1* (22), revealed an increased expression of the genes encoding for the two isoforms that were highly up-regulated in *old1–1* plants in our study, *At*GSTF7 (36- to 50-fold) and *At*GSTF2 (10- to 20-fold) (55). In light of these concordant observations in *old1–1* and *cpr5* mutants, one may reason that the *old1–1* plants undergo oxidative stress in the early stages of leaf senescence. This conclusion is supported by reports showing that in *A. thaliana* the expression of *At*GSTF6, which was found to be 5- to 10-fold up-regulated in our study, is induced by ozone (56). Ozone is generally known to trigger the biosynthesis of ethylene, a plant hormone playing a key role in leaf senescence. In carnation, elevated levels of ethylene lead to membrane degradation, lipid peroxidation, and the induction of GST genes. The role of GSTs in the context of leaf senescence is probably the protection of cells against reactive oxygen species generated by lipid degradation during the process of leaf senescence (reviewed in (24)). As mentioned above, earliest structural changes during leaf senescence consist in the disintegration of the chloroplast (19), an event that involves membrane and lipid degradation. For this reason, the presence of GSTs even in early stages of leaf senescence may be fundamental for the plant in order to maintain the functionality of the cells for efficient mobilization of the nutrients in the senescing leaf.

Serine hydroxymethyltransferase, enolase, and quinone reductase showed significant up-regulation in the *old1–1* mutant, too. To our knowledge, neither of these proteins has been associated with leaf senescence so far. As for the protein related to MLP, further studies are required to assess their significance for early leaf senescence. Interestingly, it has been hypothesized that the flavoprotein quinone reductase may have a role in the protection of plant cells from oxidative damage (25). Thus, the finding that quinone reductase is 2- to 4-fold up-regulated in the *old1–1* mutant supports our assumption that these plants experience oxidative stress during early leaf senescence.

In conclusion, our comparative, quantitative proteomics study of *A. thaliana* wt and *old1–1* mutant plants resulted in the determination of 13 distinct proteins significantly regulated in the early leaf senescence mutant. The differential regulation of some of these proteins, such as RuBisCO large and small subunits as well as some of the GST isoforms and quinone reductase, fits well into the context of early leaf senescence that had not been studied in *Arabidopsis* in such an extensive manner on the level of proteins before. However,

our list of proteins with different abundance in both *A. thaliana* phenotypes probably constitutes only a fraction of all proteins that are differentially regulated during this complex stage of leaf development. The detection of differences in rather low abundant proteins was most likely impeded by the presence of highly abundant proteins such as RuBisCO.

A promising approach for a more detailed study of proteins differentially expressed during early leaf senescence is the focused analysis of distinct sub-proteomes by employing organellar fractionation techniques, for instance. In addition, metabolic $^{14}N/^{15}N$ labeling combined with MS allows for gel-free quantitative proteomics studies facilitating the study of membrane proteins (15). Since the amino acid sequence of the OLD1 protein presumably contains an N-terminal putative nuclear localization signal and a C-terminal domain with five transmembrane regions (22, 57, 58), a quantitative organellar or membrane proteomics approach or a combination of both provide promising means to gain deeper insight into the regulation and function of this protein in (early) leaf senescence. In general, we believe that metabolic ^{15}N labeling of entire *A. thaliana* plants combined with MS for both accurate relative quantification and reliable identification of proteins provides a universal tool for comparative proteomics studies addressing a vast array of biological questions.

Acknowledgments—We thank Bernd Moritz for initializing the cooperation with the group of Jacques Hille and Klaus Jung and Sebastian Wiese for assistance with statistics and plotting.

* This study was supported by the European Graduate College 795 "Regulatory Circuits in Cellular Systems: Fundamentals and Biotechnological Applications" as well as by the Deutsche Forschungsgemeinschaft within the SFB 642 and the Bundesministerium für Bildung und Forschung. The costs of publication of this article were defrayed in part by the payment of page charges. This article must therefore be hereby marked "*advertisement*" in accordance with 18 U.S.C. Section 1734 solely to indicate this fact.

S The on-line version of this article (available at http://www.mcponline.org) contains supplemental material.

§ These authors contributed equally to this work.

‖ To whom correspondence should be addressed: Medizinisches Proteom-Center, Zentrum fuer klinische Forschung, Room E.042, Ruhr-Universitaet Bochum, Universitaetsstraβe 150, 44780 Bochum, Germany; Tel.: 49-234-32-29266; Fax: 49-234-32-14554; E-mail: bettina.warscheid@rub.de.

REFERENCES

1. Beynon, R. J., and Pratt, J. M. (2005) Metabolic labeling of proteins for proteomics. *Mol. Cell. Proteomics* **4,** 857–872
2. Julka, S., and Regnier, F. E. (2005) Recent advancements in differential proteomics based on stable isotope coding. *Brief. Funct. Genomic Proteomics* **4,** 158–177
3. Glinski, M., and Weckwerth, W. (2006) The role of mass spectrometry in plant systems biology. *Mass Spectrom. Rev.* **25,** 173–214
4. Unlu, M., Morgan, M. E., and Minden, J. S. (1997) Difference gel electrophoresis: a single gel method for detecting changes in protein extracts. *Electrophoresis* **18,** 2071–2077
5. Tonge, R., Shaw, J., Middleton, B., Rowlinson, R., Rayner, S., Young, J., Pognan, F., Hawkins, E., Currie, I., and Davison, M. (2001) Validation and development of fluorescence two-dimensional differential gel electrophoresis proteomics technology. *Proteomics* **1,** 377–396
6. Alban, A., David, S. O., Bjorkesten, L., Andersson, C., Sloge, E., Lewis, S., and Currie, I. (2003) A novel experimental design for comparative two-dimensional gel analysis: two-dimensional difference gel electrophoresis incorporating a pooled internal standard. *Proteomics* **3,** 36–44
7. Wu, W. W., Wang, G., Baek, S. J., and Shen, R. F. (2006) Comparative study of three proteomic quantitative methods, DIGE, cICAT, and iTRAQ, using 2D gel- or LC-MALDI TOF/TOF. *J. Proteome Res.* **5,** 651–658
8. Conrads, T. P., Alving, K., Veenstra, T. D., Belov, M. E., Anderson, G. A., Anderson, D. J., Lipton, M. S., Pasa-Tolic, L., Udseth, H. R., Chrisler, W. B., Thrall, B. D., and Smith, R. D. (2001) Quantitative analysis of bacterial and mammalian proteomes using a combination of cysteine affinity tags and ^{15}N-metabolic labeling. *Anal. Chem.* **73,** 2132–2139
9. Oda, Y., Huang, K., Cross, F. R., Cowburn, D., and Chait, B. T. (1999) Accurate quantitation of protein expression and site-specific phosphorylation. *Proc. Natl. Acad. Sci. U. S. A.* **96,** 6591–6596
10. Ong, S. E., Blagoev, B., Kratchmarova, I., Kristensen, D. B., Steen, H., Pandey, A., and Mann, M. (2002) Stable isotope labeling by amino acids in cell culture, SILAC, as a simple and accurate approach to expression proteomics. *Mol. Cell. Proteomics* **1,** 376–386
11. Krijgsveld, J., Ketting, R. F., Mahmoudi, T., Johansen, J., Artal-Sanz, M., Verrijzer, C. P., Plasterk, R. H., and Heck, A. J. (2003) Metabolic labeling of *C. elegans* and *D. melanogaster* for quantitative proteomics. *Nat. Biotechnol.* **21,** 927–931
12. Wu, C. C., MacCoss, M. J., Howell, K. E., Matthews, D. E., and Yates, J. R., 3rd (2004) Metabolic labeling of mammalian organisms with stable isotopes for quantitative proteomic analysis. *Anal. Chem.* **76,** 4951–4959
13. Gruhler, A., Schulze, W. X., Matthiesen, R., Mann, M., and Jensen, O. N. (2005) Stable isotope labeling of *Arabidopsis thaliana* cells and quantitative proteomics by mass spectrometry. *Mol. Cell. Proteomics* **4,** 1697–1709
14. Engelsberger, W. R., Erban, A., Kopka, J., and Schulze, W. X. (2006) Metabolic labeling of plant cell cultures with $K^{15}NO_3$ as a tool for quantitative analysis of proteins and metabolites. *Plant Methods 2,* **14,** 1–11
15. Lanquar, V., Kuhn, L., Lelievre, F., Khafif, M., Espagne, C., Bruley, C., Barbier-Brygoo, H., Garin, J., and Thomine, S. (2007) ^{15}N-metabolic labeling for comparative plasma membrane proteomics in *Arabidopsis* cells. *Proteomics* **7,** 750–754
16. Huttlin, E. L., Hegeman, A. D., Harms, A. C., and Sussman, M. R. (2007) Comparison of full versus partial metabolic labeling for quantitative proteomics analysis in *Arabidopsis thaliana. Mol. Cell. Proteomics* **6,** 860–881
17. Benschop, J. J., Mohammed, S., O'Flaherty, M., Heck, A. J., Slijper, M., and Menke, F. L. (2007) Quantitative phospho-proteomics of early elicitor signalling in *Arabidopsis. Mol. Cell. Proteomics* **6,** 1198–1214
18. Nelson, C. J., Huttlin, E. L., Hegeman, A. D., Harms, A. C., and Sussman, M. R. (2007) Implications of ^{15}N-metabolic labeling for automated peptide identification in *Arabidopsis thaliana. Proteomics* **7,** 1279–1292
19. Lim, P. O., Kim, H. J., and Nam, H. G. (2006) Leaf senescence. *Annu. Rev. Plant Biol.* **58,** 115–136
20. Jing, H. C., Sturre, M. J. G., Hille, J., and Dijkwel, P. P. (2002) *Arabidopsis* onset of leaf death mutants identify a regulatory pathway controlling leaf senescence. *Plant J.* **32,** 51–63
21. Jing, H. C., Schippers, J. H., Hille, J., and Dijkwel, P. P. (2005) Ethylene-induced leaf senescence depends on age-related changes and OLD genes in *Arabidopsis. J. Exp. Bot.* **56,** 2915–2923
22. Jing, H. C., Anderson, L., Sturre, M. J. G., Hille, J., and Dijkwel, P. P. (2007) *Arabidopsis* CPR5 is a senescence-regulatory gene with pleiotropic function as predicted by the evolutionary theory of senescence. *J. Exp. Bot., in press*
23. Kolkman, A., Dirksen, E. H., Slijper, M., and Heck, A. J. (2005) Double standards in quantitative proteomics: direct comparative assessment of difference in gel electrophoresis and metabolic stable isotope labeling. *Mol. Cell. Proteomics* **4,** 255–266
24. Marrs, K. A. (1996) The functions and regulation of glutathione S-transferases in plants. *Annu. Rev. Plant Physiol. Plant Mol. Biol.* **47,** 127–158
25. Sparla, F., Tedeschi, G., Pupillo, P., and Trost, P. (1999) Cloning and heterologous expression of NAD(P)H:quinone reductase of *Arabidopsis thaliana*, a functional homologue of animal DT-diaphorase. *FEBS Lett.* **463,** 382–386
26. Hoagland, D. R., and Snyder, W.C. (1933) Nutrition of strawberry plants under controlled conditions. *Proc. Am. Soc. Hort. Sci.* **30,** 288–294

27. Giavalisco, P., Nordhoff, E., Lehrach, H., Gobom, J., and Klose, J. (2003) Extraction of proteins from plant tissues for two-dimensional electrophoresis analysis. *Electrophoresis* **24,** 207–216
28. Cohen, S. A., and Michaud, D. P. (1993) Synthesis of a fluorescent derivatizing reagent, 6-aminoquinolyl-N-hydroxysuccinimidyl carbamate, and its application for the analysis of hydrolysate amino acids via high-performance liquid chromatography. *Anal. Biochem.* **211,** 279–287
29. Cohen, S. A., and De Antonis, K. M. (1994) Applications of amino acid derivatization with 6-aminoquinolyl-N-hydroxysuccinimidyl carbamate: analysis of feed grains, intravenous solutions and glycoproteins. *J. Chromatogr. A* **661,** 25–34
30. Klose, J. (1975) Protein mapping by combined isoelectric focusing and electrophoresis of mouse tissues: a novel approach to testing for induced point mutations in mammals. *Humangenetik* **26,** 231–243
31. Klose, J., and Kobalz, U. (1995) Two-dimensional electrophoresis of proteins: an updated protocol and implications for a functional analysis of the genome. *Electrophoresis* **16,** 1034–1059
32. Neuhoff, V., Stamm, R., Pardowitz, I., Arold, N., Ehrhardt, W., and Taube, D. (1990) Essential problems in quantification of proteins following colloidal staining with Coomassie brilliant blue dyes in polyacrylamide gels, and their solution. *Electrophoresis* **11,** 101–117
33. Schaefer, H., Chervet, J. P., Bunse, C., Joppich, C., Meyer, H. E., and Marcus, K. (2004) A peptide preconcentration approach for nano-high-performance liquid chromatography to diminish memory effects. *Proteomics* **4,** 2541–2544
34. Eng, J. K., McCormack, A. L., and Yates, J. R. (1994) An approach to correlate tandem mass spectral data of peptides with amino acid sequences in a protein database. *J. Am. Soc. Mass Spectrom.* **5,** 976–989
35. Ducret, A., Van Oostveen, I., Eng, J. K., Yates, J. R., 3rd, and Aebersold, R. (1998) High throughput protein characterization by automated reverse-phase chromatography/electrospray tandem mass spectrometry. *Protein Sci.* **7,** 706–719
36. Boehm, A. M., Galvin, R. P., and Sickmann, A. (2004) Extractor for ESI quadrupole TOF tandem MS data enabled for high throughput batch processing. *BMC Bioinformatics 5,* **162,** 1–5
37. Taylor, J. R. (1997) *An Introduction to Error Analysis: The Study of Uncertainties in Physical Measurements*, 2nd Ed., University Science Books, New York
38. Tukey, J. W. (1990) Data-based graphics: visual display in the decades to come. *Statist. Sci.* **5,** 327–339
39. Motulsky, H. (1995) *Intuitive Biostatistics*, Oxford University Press, New York
40. Wang, Y. K., Ma, Z., Quinn, D. F., and Fu, E. W. (2002) Inverse ^{15}N-metabolic labeling/mass spectrometry for comparative proteomics and rapid identification of protein markers/targets. *Rapid Commun. Mass Spectrom.* **16,** 1389–1397
41. Marouga, R., David, S., and Hawkins, E. (2005) The development of the DIGE system: 2D fluorescence difference gel analysis technology. *Anal. Bioanal. Chem.* **382,** 669–678
42. Edwards, R., Dixon, D. P., and Walbot, V. (2000) Plant glutathione S-transferases: enzymes with multiple functions in sickness and in health. *Trends Plant Sci.* **5,** 193–198
43. Wagner, U., Edwards, R., Dixon, D. P., and Mauch, F. (2002) Probing the diversity of the *Arabidopsis* glutathione S-transferase gene family. *Plant Mol. Biol.* **49,** 515–532
44. Li, X. J., Zhang, H., Ranish, J. A., and Aebersold, R. (2003) Automated statistical analysis of protein abundance ratios from data generated by stable-isotope dilution and tandem mass spectrometry. *Anal. Chem.* **75,** 6648–6657
45. Hortensteiner, S., and Feller, U. (2002) Nitrogen metabolism and remobilization during senescence. *J. Exp. Bot.* **53,** 927–937
46. Cannon, S. B., and Young, N. D. (2003) OrthoParaMap: distinguishing orthologs from paralogs by integrating comparative genome data and gene phylogenies. *BMC Bioinformatics* **35,** 1–15
47. Stromvik, M. V., Sundararaman, V. P., and Vodkin, L. O. (1999) A novel promoter from soybean that is active in a complex developmental pattern with and without its proximal 650 base pairs. *Plant Mol. Biol.* **41,** 217–231
48. Frova, C. (2003) The plant glutathione transferase gene family: genomic structure, functions, expression and evolution. *Physiol. Plant.* **119,** 469–479
49. Moons, A. (2005) Regulatory and functional interactions of plant growth regulators and plant glutathione S-transferases (GSTs). *Vitam. Horm.* **72,** 155–202
50. Smith, A. P., DeRidder, B. P., Guo, W. J., Seeley, E. H., Regnier, F. E., and Goldsbrough, P. B. (2004) Proteomic analysis of *Arabidopsis glutathione* S-transferases from benoxacor- and copper-treated seedlings. *J. Biol. Chem.* **279,** 26098–26104
51. Guo, J., Cai, Z., and Gan, S. (2004) Transcriptome of *Arabidopsis* leaf senescence. *Plant, Cell Environment* **27,** 521–549
52. Jepson, I., Lay, V. J., Holt, D. C., Bright, S. W., and Greenland, A. J. (1994) Cloning and characterization of maize herbicide safener-induced cDNAs encoding subunits of glutathione S-transferase isoforms I, II and IV. *Plant Mol. Biol.* **26,** 1855–1866
53. Buchanan-Wollaston, V., Page, T., Harrison, E., Breeze, E., Lim, P. O., Nam, H. G., Lin, J. F., Wu, S. H., Swidzinski, J., Ishizaki, K., and Leaver, C. J. (2005) Comparative transcriptome analysis reveals significant differences in gene expression and signalling pathways between developmental and dark/starvation-induced senescence in *Arabidopsis. Plant J.* **42,** 567–585
54. Zimmermann, P., Hirsch-Hoffmann, M., Hennig, L., and Gruissem, W. (2004) *GENEVESTIGATOR: Arabidopsis* microarray database and analysis toolbox. *Plant Physiol.* **136,** 2621–2632
55. Zimmermann, P., Hennig, L., and Gruissem, W. (2005) Gene-expression analysis and network discovery using Genevestigator. *Trends Plant Sci.* **10,** 407–409
56. Sharma, Y. K., and Davis, K. R. (1994) Ozone-induced expression of stress-related genes in *Arabidopsis thaliana. Plant Physiol.* **105,** 1089–1096
57. Yoshida, S., Ito, M., Nishida, I., and Watanabe, A. (2002) Identification of a novel gene HYS1/CPR5 that has a repressive role in the induction of leaf senescence and pathogen-defence responses in *Arabidopsis thaliana. Plant J.* **29,** 427–437
58. Kirik, V., Bouyer, D., Schobinger, U., Bechtold, N., Herzog, M., Bonneville, J. M., and Hulskamp, M. (2001) CPR5 is involved in cell proliferation and cell death control and encodes a novel transmembrane protein. *Curr. Biol.* **11,** 1891–1895